Supplement of Biogeosciences, 23, 2939–2958, 2026
https://doi.org/10.5194/bg-23-2939-2026-supplement

Biogeosciences
Open Access

Supplement of

Dissolved oxygen budget in the Levantine Sea: a coupled physical-biogeochemical modelling approach

Joelle Habib et al.

Correspondence to: Joelle Habib (joellehabib22@hotmail.com)

Supplement Material

S1: Equation of dissolved oxygen budget

The variation of the dissolved oxygen inventory in the upper layer between times t_1 and t_2 ($\Delta\ DOx\ I_{upper}$), in mol $O_2\ m^{-2}$, is equal to the sum of all DOx fluxes within the Levantine Basin between t_1 and t_2:

$$\Delta\ DOx\ I_{upper} = DOx\ I_{upper,\ t1} - DOx\ I_{upper,t2} = \int_{t_1}^{t_2} \left(F_{DOx,air-sea} + F_{DOx,lat} + F_{DOx,vert} + F_{DOx,bgc} \right) dt \quad (S1)$$

where $F_{DOx,lat,}$ and $F_{DOx,vert}$ are the lateral and vertical fluxes at the boundaries of the Levantine Basin area, $F_{DOx,air-sea}$ is the air-sea flux, and $F_{DOx,bgc}$ is the biogeochemical flux.

$DOx\ I_{upper,t}$ was computed from:

$$DOx\ I_{upper,t} = \int\int \int_{(x,y)\in RG/z\in upper\ layer} DOx(x,y,z,t)\ dx\ dy\ dz \quad (S2)$$

where (x,y,z) belongs to the upper layer (150 m to the surface) of the Levantine Basin.

The lateral flux was computed from:

$$F_{DOx,lat} = \int\int_A DOx(x,y,z,t)\ v_t(x,y,z,t)\ dA \quad (S3)$$

where v_t is the current velocity normal to the limits of the Levantine Basin (in $m^3\ s^{-1}$), and A is the area of the section from the base of the upper layer (150 m) to the surface. We distinguished the limit with the Ionian Sea and the one with the Aegean Sea (indicated in Fig. 1).

$F_{DOx,bgc}$ was computed from:

$$F_{DOx,bgc} = \int \int_{(x,y)\in RG\ /\ z\ \in\ upper\ layer} \int BGCflux(x,y,z,t)\ dx\ dy\ dz \quad (S4)$$

where *BGCflux* is the biogeochemical flux, i.e. $\gamma_{C/DOx}$ GPP - $\gamma_{C/DOx}$ CR - $\gamma_{N/DOx}$ Nitrif, where GPP is the gross primary production, CR, the community respiration, and Nitrif the nitrification.
Finally, the vertical transport flux, $F_{DOx,vert}$, was derived from all other terms of Eq. (S1).

The computation of DOx balance in the intermediate layer is computed similarly, with the inventory variation as the sum of the lateral and vertical fluxes at the boundaries, and the biogeochemical flux.

Tables

Table S1: Comparison between averaged modeled and observation rates over the same period and along the same region. a: Lagaria et al., (2011), b: Christaki et al. (2011), c: Regaudie-de-Gioux et al. (2009), (d) Moutin and Raimbault (1996).

Process	Campaign	Region	Period	Layer	Observation	Model	Reference
GPP	BOUM	Core of an anticyclonic eddy in the eastern Levantine	mid-June to mid-July	Near the surface	0.12 ± 0.90 mmol O_2 m^{-3} day^{-1}	1.36 mmol O_2 m^{-3} day^{-1}	a
				Integrated 145 m	28-75 mmol O_2 m^{-2} day^{-1}	68 mmol O_2 m^{-2} day^{-1}	b
	THRESHOLD	Levantine Basin	May	5-110 m	0.16-2.93 mmol O_2 m^{-3} day^{-1}	1-8 mmol O_2 m^{-3} day^{-1}	c
	MINOS	Levantine Basin	May to June	Near the surface	0.59 ± 0.16 mmol O_2 m^{-3} day^{-1}	1.08 mmol O_2 m^{-3} day^{-1}	d
			May to June	Integrated 100m	37.9 ± 4.8 mmol O_2 m^{-2} day^{-1}	37 mmol O_2 m^{-2} day^{-1}	d
CR	BOUM	Core of an anticyclonic eddy in the eastern Levantine	mid-June to mid-July	Near the surface	0.38 ± 0.92 mmol O_2 m^{-3} day^{-1}	1.28 mmol O_2 m^{-3} day^{-1}	a
				Integrated 145 m	39-58 mmol O_2 m^{-2} day^{-1}	68 mmol O_2 m^{-2} day^{-1}	b
	THRESHOLD	Levantine Basin	May	5-110 m	0.1-8.2 mmol O_2 m^{-3} day^{-1}	1-7 mmol O_2 m^{-3} day^{-1}	c
NCP	BOUM	Core of an anticyclonic eddy in the eastern Levantine	mid-June to mid-July	Near the surface	-0.26 ± 0.22 mmol O_2 m^{-3} day^{-1}	0.09 mmol O_2 m^{-3} day^{-1}	a
				Integrated 145 m	4 ± 15 mmol O_2 m^{-2} day^{-1}	0.9 mmol O_2 m^{-2} day^{-1}	b
	THRESHOLD	Levantine Basin	May	5-110 m	-6.4-8.2 mmol O_2 m^{-3} day^{-1}	0-2 mmol O_2 m^{-3} day^{-1}	c

Table S2: Metrics computed for MLD and heat flux for the Levantine basin for 2013-2020 winter (December-January-February). Blue columns represent the cold winter years.

	Units	2013-14	2014-15	2015-16	2016-17	2017-18	2018-19	2019-20	2020-21	Mean (SD)
Mean winter heat flux	W m^{-2}	-121	-169	-137	-177	-124	-182	-168	-132	-152 (25)
Maximum MLD	m	95	123	107	121	107	112	105	92	108 (11)
Date of maximum MLD	-	4 Feb	20 Feb	25 Jan	28 Jan	26 Jan	16 Jan	9 Feb	18 Feb	-
Mean MLD	m	70	76	67	83	71	83	69	59	72 (8)
Mean Wind stress	N m^{-2}	0.010	0.024	0.018	0.016	0.016	0.03	0.022	0.014	0.019

Table S3: Annual air-sea oxygen flux, biogeochemical oxygen flux, and vertical oxygen flux at 150 and 400 m for the different years and averaged over the 7 years, estimated from the model in the Levantine basin. Positive values correspond to an input for the study area. The annual budget is calculated from December. The numbers in bold represent the cold winter years.

		Units	2013-14	**2014-15**	2015-16	**2016-17**	2017-18	**2018-19**	2019-20	Mean
Surface layer (0 -150 m)	Internal variation	Mol m^{-2}	-0.23	**0.31**	-0.22	**0.06**	-0.22	**0.36**	-0.32	-0.03 (0.28)
	Air-sea flux	Mol m^{-2}	0.7	**2.11**	0.96	**2.11**	0.89	**2.15**	1.26	1.45 (0.6)
	BGC	Mol m^{-2}	-0.17	**0.34**	0.11	**0.4**	-0.06	**0.46**	0.08	0.2 (0.2)
	NCP	Mol m^{-2}	0.82	**1.39**	1.15	**1.5**	1.06	**1.6**	1.2	1.23 (2.95)
	Physical transfer	Mol m^{-2}	-0.76	**-2.15**	-1.29	**-2.46**	-1.05	**-2.25**	-1.67	-1.66 (0.65)
	Downward flux at 150 m	Mol m^{-2}	-3.89	**-6.18**	-3.91	**-3.94**	-2.91	**-4.98**	-3.46	-4.2 (1.1)
	Lat Ionian flux	Mol m^{-2}	9.13	**14.0**	9.92	**11.78**	11.2	**14.38**	10.07	11.5 (2)
	Lat Aegean flux	Mol m^{-2}	-6.00	**-9.98**	-7.31	**-10.31**	-9.34	**-11.65**	-8.29	-9 (1.9)
	Internal variation	Mol m^{-2}	-0.19	**0.80**	-0.06	**0.24**	-0.03	**0.72**	-0.08	0.22 (0.4)
	BGC	Mol m^{-2}	-1.62	**-2.24**	-1.89	**-2.23**	-1.65	**-2.33**	-1.95	-2 (0.3)

Intermediate layer (150 - 400 m)	Physical transfer	Mol m^{-2}	1.45	**3.04**	1.84	**2.48**	1.62	**3.05**	1.86	2.19 (0.66)
	vertical flux at 400 m	Mol m^{-2}	0.58	**-0.95**	0.37	**1.22**	-0.58	**-0.04**	0.99	0.22 (0.79)
	Vertical flux net	Mol m^{-2}	4.47	**5.24**	4.28	**5.16**	2.33	**4.94**	4.45	4.4 (0.99)
	Lat Ionian flux	Mol m^{-2}	-1.41	**1.4**	-1.01	**2.46**	2.18	**3.76**	0.2	1.1 (1.9)
	Lat Aegean flux	Mol m^{-2}	-1.61	**-3.60**	-1.43	**-5.14**	-2.89	**-5.65**	-2.79	-3.3 (1.6)

Table S4: Annual air-sea oxygen flux, biogeochemical oxygen flux, vertical oxygen flux at 150 and 400 m, and lateral oxygen flux averaged over the 7 years, estimated from the model in the Rhodes Gyre. Positive values correspond to an input for the study area. The annual budget is calculated from December.

		Surface (0-150m)	Intermediate (150-400m)		Surface (0-150m)	Intermediate (150-400m)
Internal variation	Mol m^{-2} yr^{-1}	0.01 (0.3)	0.26 (0.39)	Gmol yr^{-1}	0.3 (8)	7 (10.8)
Air-sea flux	Mol m^{-2} yr^{-1}	3.92 (1.7)	-	Gmol yr^{-1}	108 (49)	-
BGC	Mol m^{-2} yr^{-1}	1.34 (0.56)	-1.08 (0.33)	Gmol yr^{-1}	37 (15)	-30 (9)
Physical transfer	Mol m^{-2} yr^{-1}	-5.25 (2)	1.35 (0.7)	Gmol yr^{-1}	-144 (57)	37 (19)
Vertical flux	Mol m^{-2} yr^{-1}	4.15 (4.3)	6.98 (2.7)	Gmol yr^{-1}	114 (119)	192 (75)
Lateral flux	Mol m^{-2} yr^{-1}	-9.4 (3.11)	-5.63 (2.3)	Gmol yr^{-1}	-258 (85)	-155 (63)

Figures

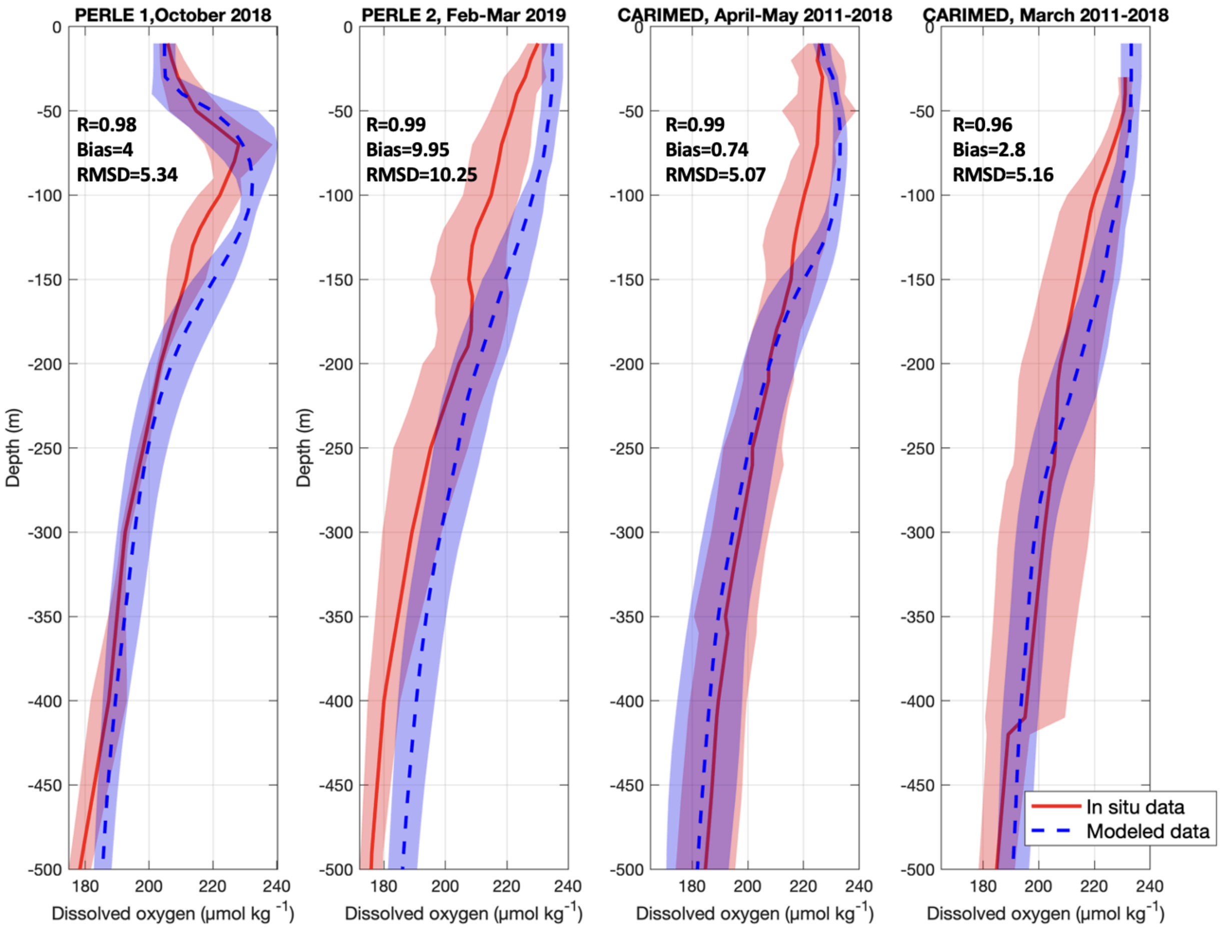

Figure S1: Comparison between the mean modeled (blue dotted line) and observed (red solid line) profiles of the dissolved oxygen concentration (μmol O_2 kg^{-1}) during (a) PERLE-1, 6 profiles (10-20 October 2018), (b) PERLE-2, 16 profiles (25 February-16 March 2019), and CARIMED, 29 profiles (2011-2018) cruises occurring (c) during the stratification and (d) during mixing period. The shaded areas represent the standard deviation over the different profiles. Coefficient correlation (R), bias, and RMSD between model outputs and observations are indicated in the figures.

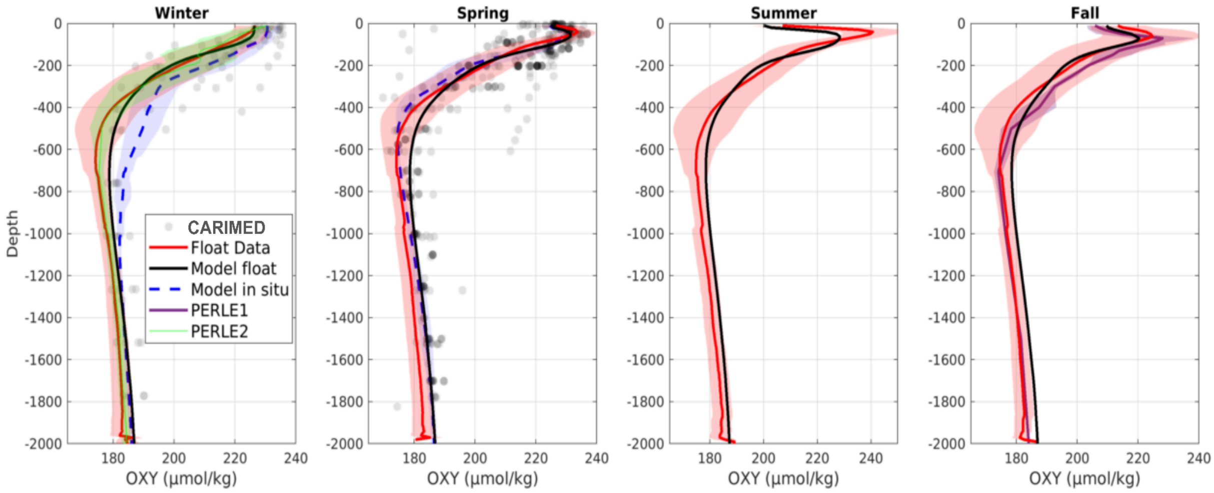

Figure S2: Comparison between observed (CARIMED, BGC-Argo float, PERLE-1, and PERLE-2 data, grey dots, red, purple, and green lines) and modeled (black and blue lines) profiles of oxygen (µmol kg^{-1}) concentrations, averaged by season (winter: 21 December to 20 March, spring: 21 March to 20 June, summer: 21 June to 20 September, fall: 21 September to 20 December), over the Levantine Sea. Shaded areas correspond to SD.

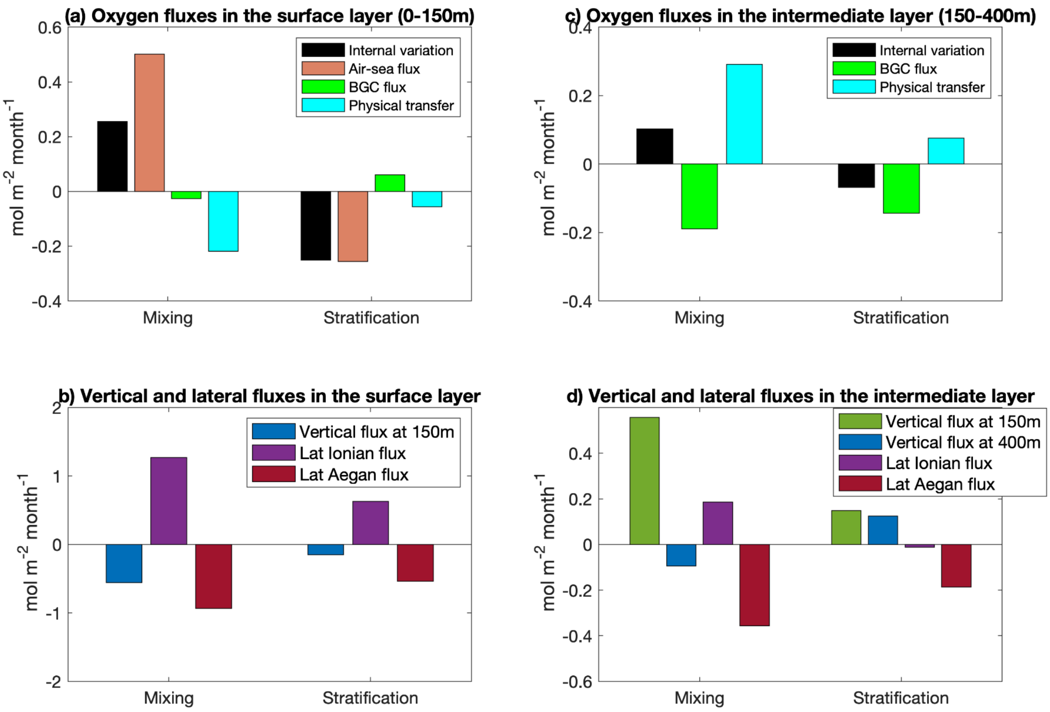

Figure S3: Modeled seasonal oxygen fluxes (a) in the surface and (c) intermediate layers and the downward and lateral fluxes (b) in the surface and (d) intermediate layers for the period of study, 2013-2020, and the Levantine Basin. Note that the y-axis range varies for the different figures.

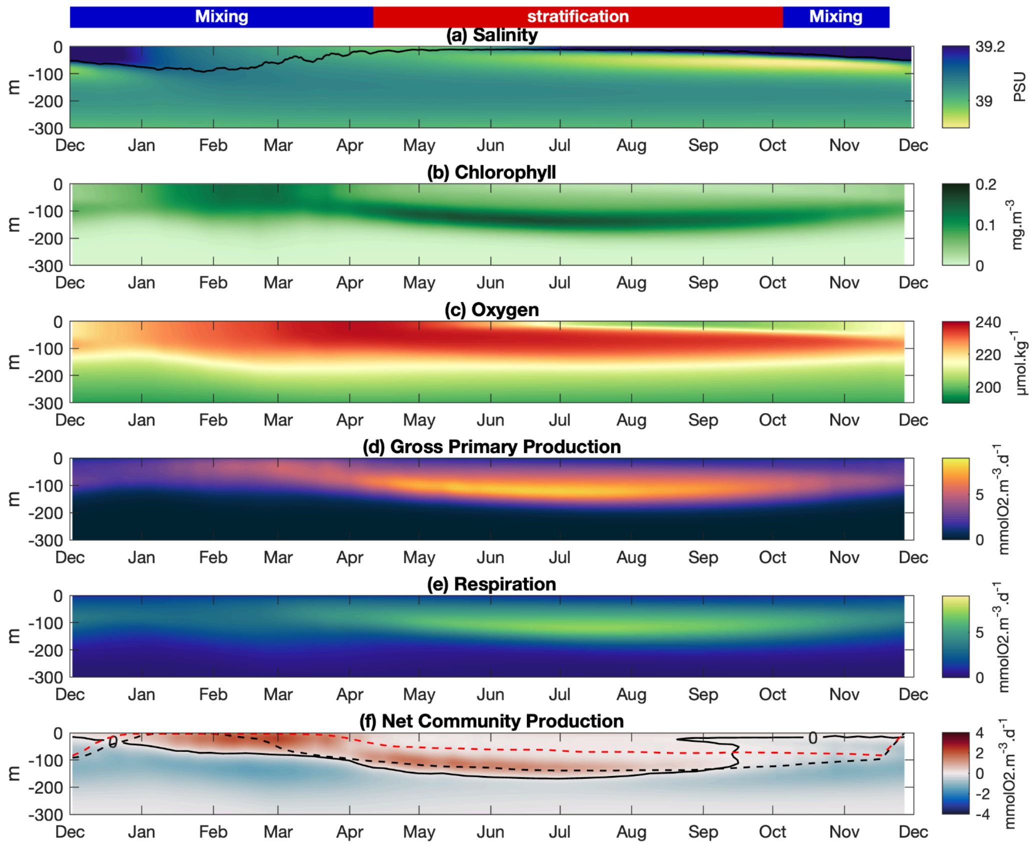

Fig. S4: Hovmöller diagrams of (a) salinity, (b) chlorophyll (mg m^{-3}), (c) dissolved oxygen concentration (µmol kg^{-1}), (d) gross primary production (mmol m^{-2} day^{-1}), (e) community respiration (mmol m^{-2} day^{-1}), and (f) net community production (mmol m^{-2} day^{-1}), averaged over the Levantine Basin, from December 2013 to May 2021. The black line in (a) indicates the mixed layer depth.

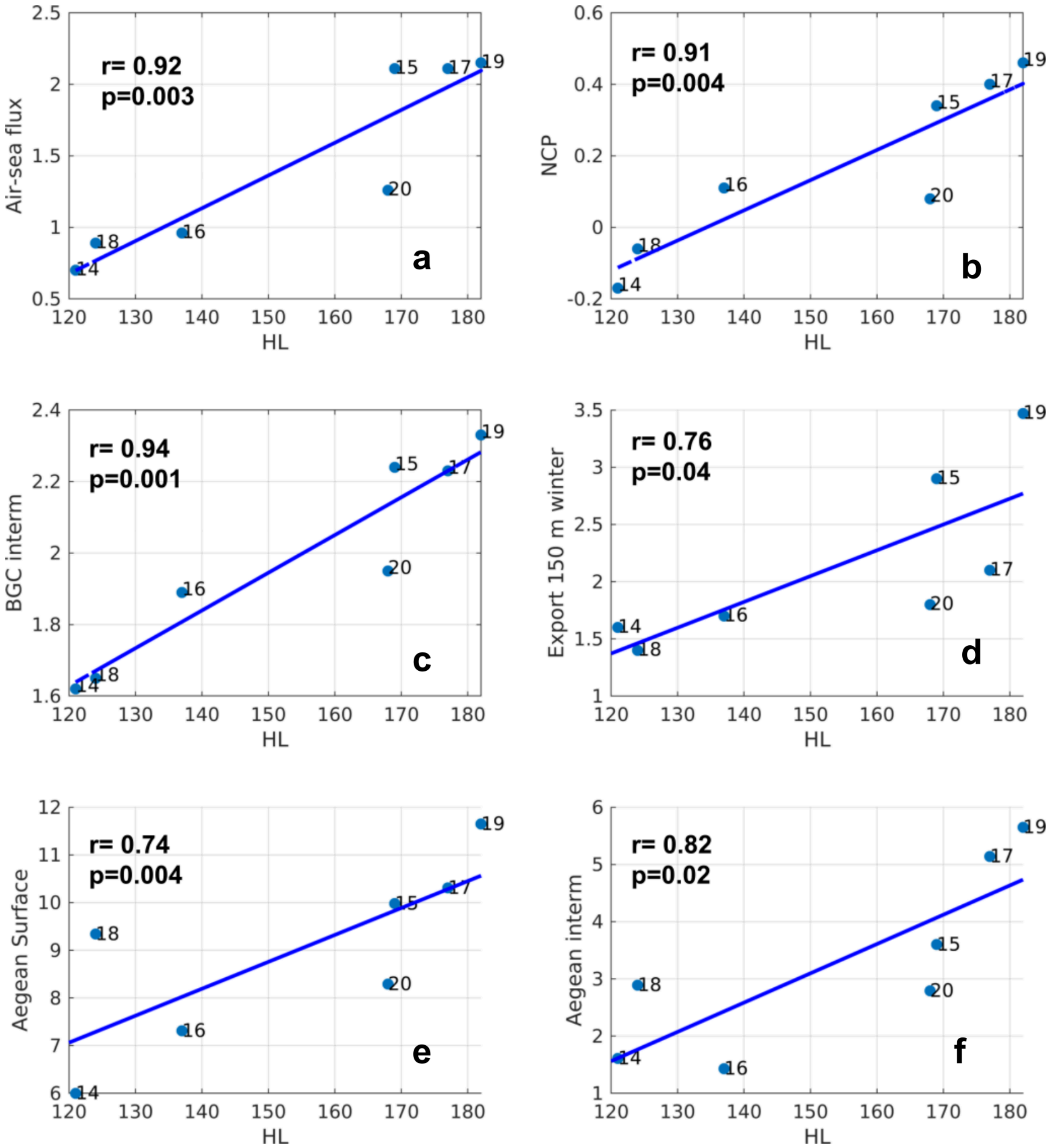

Figure S5: Scatter-plot of winter heat loss (W m^{-2}) vs. mean annual values of (a) Air-sea oxygen flux (mol m^{-2}) into surface layer (b) NCP (mol m^{-2}), (c) biogeochemical consumption in the intermediate layer, (d) winter downward export of oxygen at 150 m, (e) lateral oxygen export towards the Aegean in the surface layer, and (f) in the intermediate layer. The years are identified by the numbers in black, e.g., 14 stands for 2013-14. The blue line shows the linear regression over the 7 years. The corresponding correlations and p-values are shown for each variable.

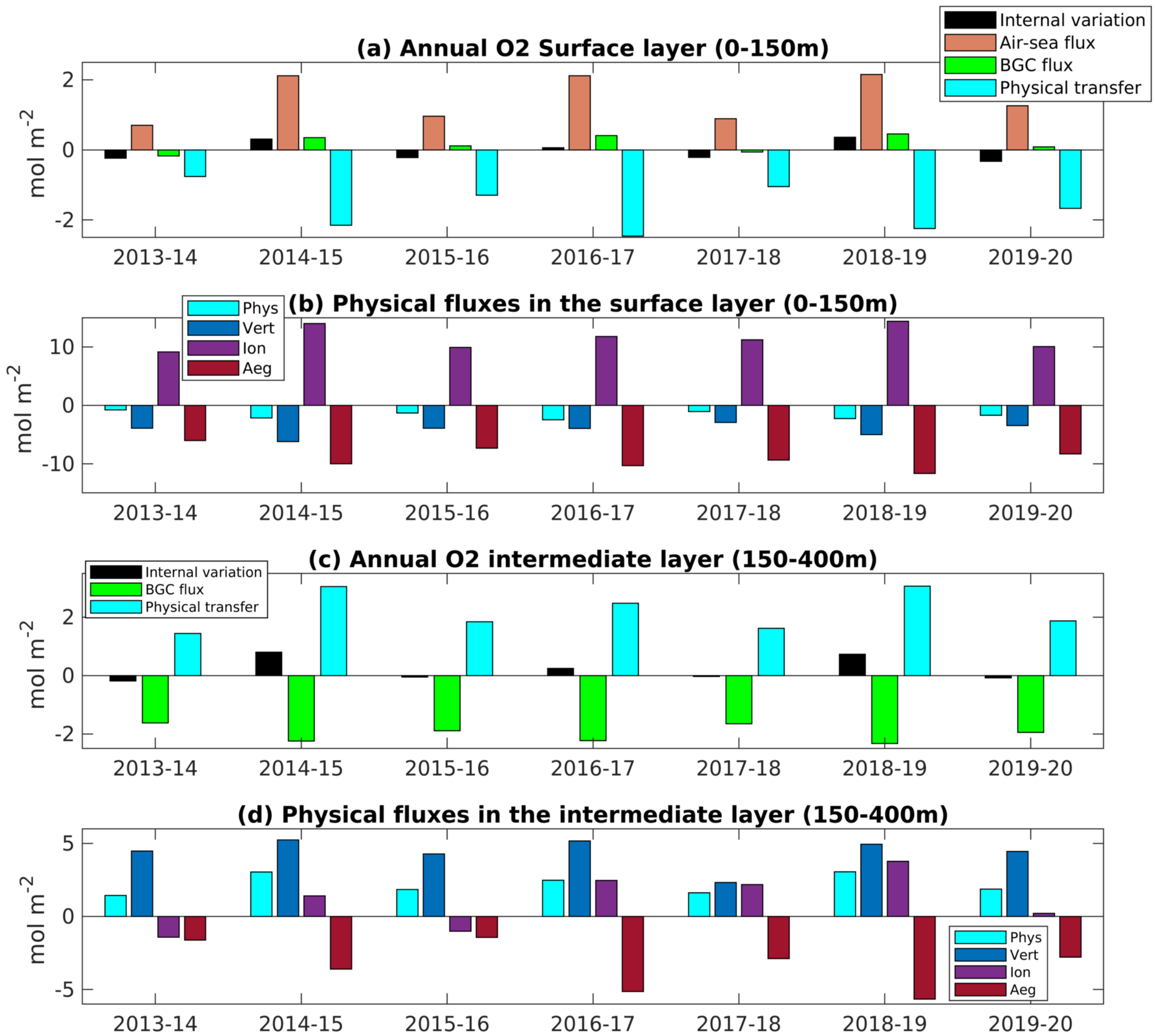

Figure S6: (a) Modeled annual dissolved oxygen fluxes (b) and the detailed vertical and lateral transport at the limits of the 0-150 m layer. (c) Modeled annual dissolved oxygen fluxes (d) and the detailed vertical and lateral transport at the limits of the 150 -400 m layer.

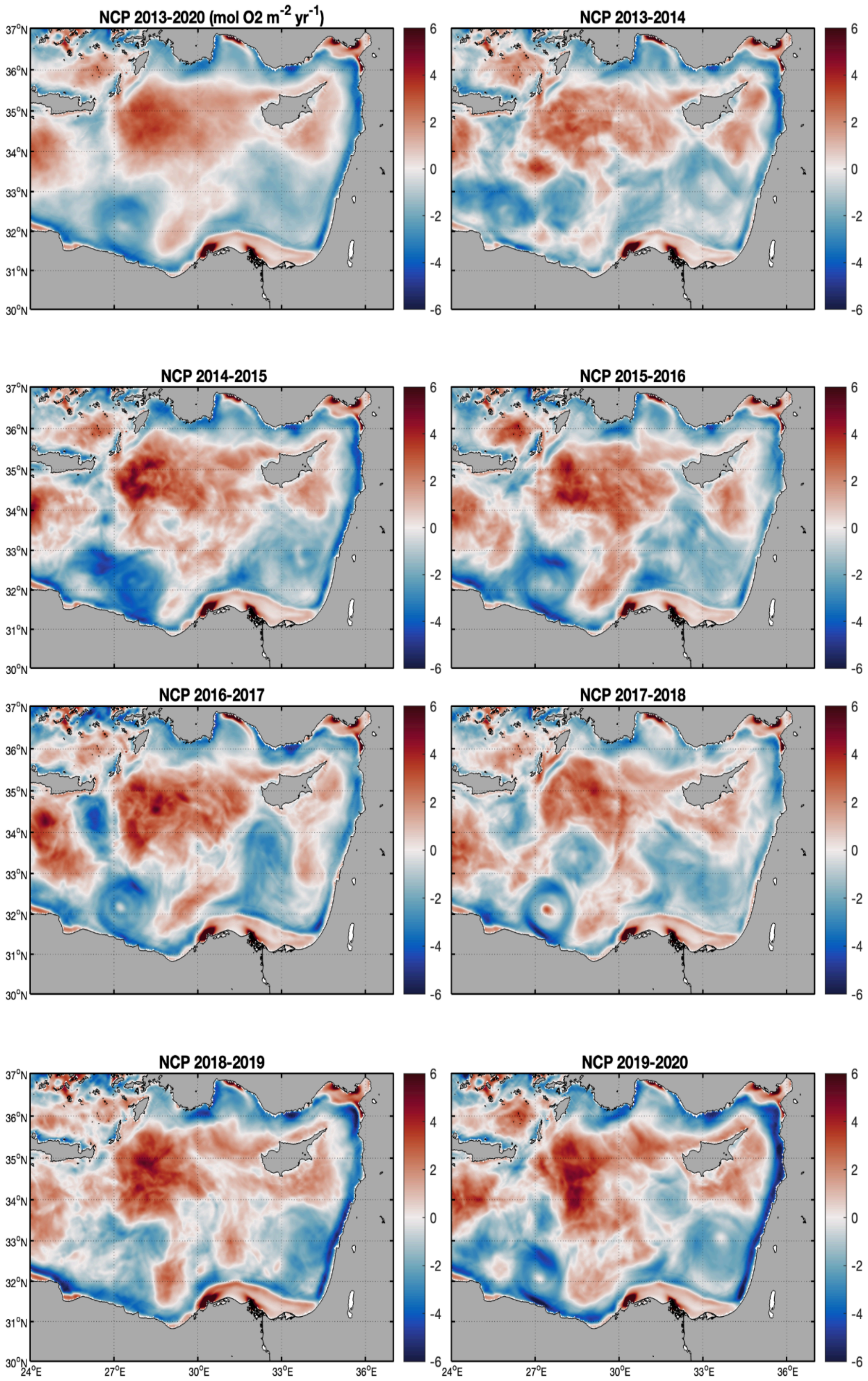

Figure S7: Modeled annual net community production (NCP) in the surface layer (0-150 m) for the period from December 2013 to December 2020.

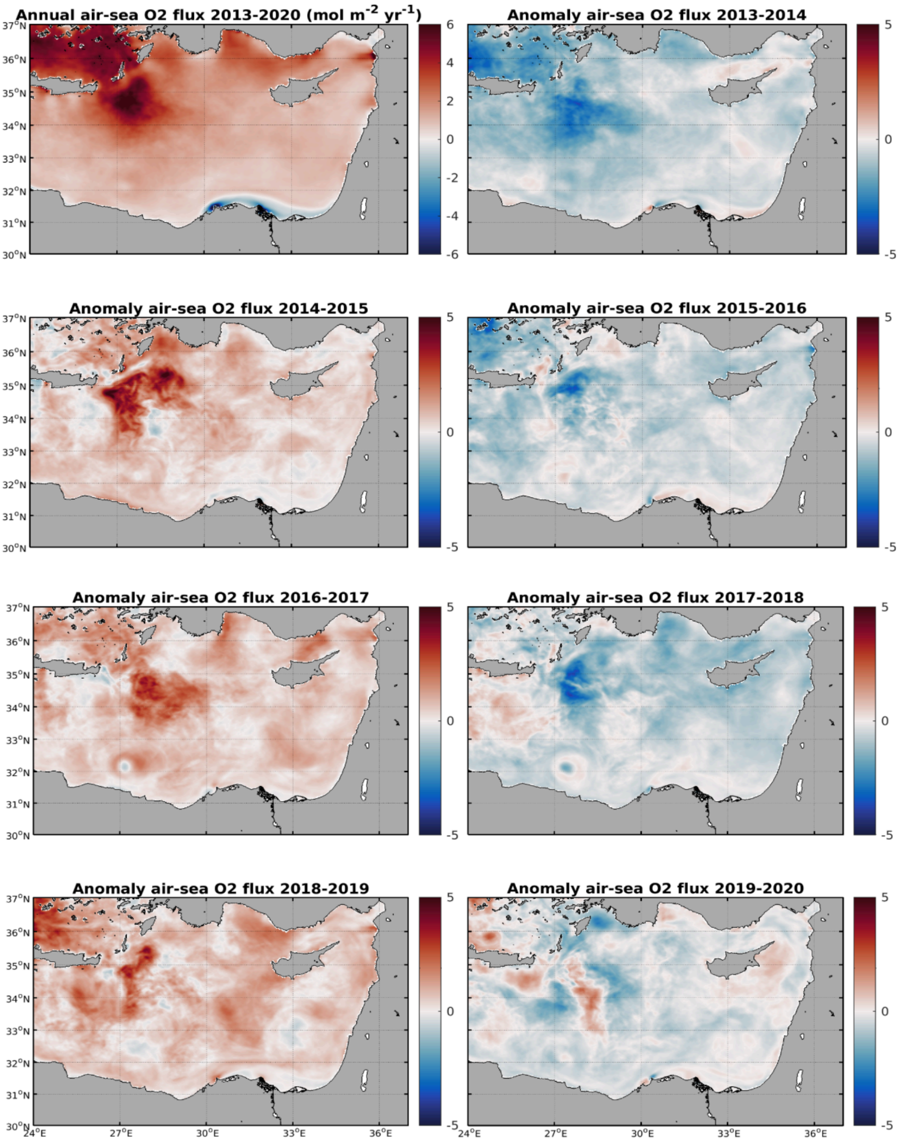

Figure S8: Modeled annual air-sea oxygen flux in the surface layer (0-150 m) for the period from December 2013 to December 2020.